Bioconjugate Chemistry

Article

pubs.acs.org/bc

Comb-Like Oligoaminoethane Carriers: Change in Topology Improves pDNA Delivery

Claudia Scholz, Petra Kos, and Ernst Wagner*

Pharmaceutical Biotechnology, Center for System-based Drug Research and Center for NanoScience (CeNS), Ludwig-Maximilians-Universität, Butenandtstrasse 5-13, 81377 Munich, Germany

Supporting Information

ABSTRACT: Establishing precise structure−activity relationships is important for the optimization of synthetic carriers for gene delivery. Sequence-defined oligomers with branched or linear shapes were synthesized to investigate the influence of topology on their biophysical properties and biological performance. Comb-like structures were synthesized consisting of an oligolysine peptide backbone modified at the ε-amino groups with four different artificial oligoamino acids, succinyl-diethylene triamine (Sdt), succinyl-triethylene tetramine (Stt), succinyl-tetraethylene pentamine (Stp), and succinyl-pentaethylene hexamine (Sph). Optionally the amino acids histidine and alanine were inserted into the oligolysine backbone to assess a possible buffer or spacer effect. After the evaluation of biophysical properties, the best performing oligomers, containing the Stp or Sph building blocks, were compared to corresponding linear oligomers where Stp or Sph are directly integrated into the linear oligolysine row. Clear differences between the comb and linear carriers were observed in the comparison of properties such as DNA complexation ability, buffer capacity, cellular association and internalization, and gene transfer. For the Stp containing structures, the comb topology mediated an increased buffer capacity at endosomal pH. For the Sph containing structures, in sharp contrast, the linear topology displayed advantageous endosomal buffering. Interestingly, for both Stp and Sph carriers, the comb in comparison to the linear topologies mediated a higher overall cellular uptake despite a lower cell association. For Stp combs, the combined advantage in both buffering and cellular uptake resulted in a strong (10- to >100-fold) increase in DNA transfection efficiency. In the case of Sph carriers, comb topology mediated only moderately (maximum 4-fold) enhanced gene transfer over the linear topology.

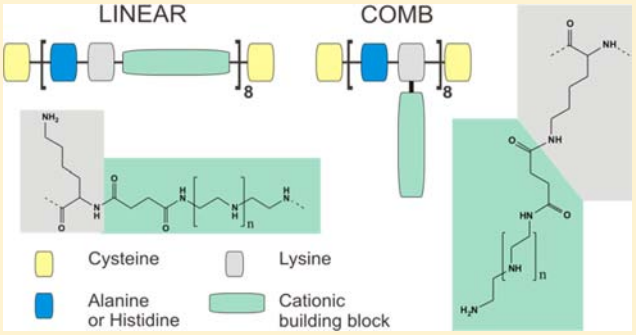

INTRODUCTION

Gene therapy has become a promising tool for the cure of several diseases like cancer and other genetic dysfunctions. Despite remarkable advances in this area, various drawbacks concerning safety and effectiveness have maintained the need for optimization of therapeutic concepts for clinical application. Cationic polymers have gained more and more importance as synthetic carriers for nucleic acid delivery, with polyethylenimine (PEI)[1−3] as a prominent example. More recently, in order to overcome the main disadvantage of PEI as a polydisperse polymer with significant toxicity,[4−6] novel analogs containing defined smaller chemical ethylenimine units were designed.[7−13] For example, the diaminoethane motif was introduced into the artificial amino acid succinyl-tetraethylene-pentamine (Stp).[14] This motif was found to be effective for nucleic acid binding and endosomal buffering and thus provides the basis for the production of precise, sequence-defined carriers.[15−21]

The importance of carrier topology for the purpose of modulating their biophysical properties and biological performance has previously been recognized.[22,23] Differences in biophysical properties and in the transfection efficiency of branched and linear PEI have been shown in several studies.[22,23] A study using poly(amido amine)s with different branched architectures reported an improved DNA compaction ability and buffer capacity and therefore enhanced transfection efficiency with increasing degree of branching.[24] Several studies have investigated the effect of varying the length of oligoamine moieties in polymeric carriers on biophysical properties, buffer capacity, and especially nucleic acid transfection efficiency.[20,25−27] Significant effects of the number and type of amines, total amine density, and spacer length between the amino groups underline the importance of investigating structure−activity relationships for the optimization of carrier design.

In this study we present the synthesis and biological application of new comb-like cationic oligomers. In contrast to our recent previous work, the different diaminoethane building blocks are not part of the polymer backbone but are attached to the ε-amino groups of an oligolysine peptide backbone, thus forming tiny branches, like teeth of a comb. The

Received: August 23, 2013
Revised: December 17, 2013
Published: December 20, 2013

artificial amino acids tested as branches in this study were succinyl-diethylene triamine (Sdt), succinyl-triethylene tetramine (Stt), succinyl-tetraethylene pentamine (Stp), and succinyl-pentaethylene hexamine (Sph) providing two to five protonatable amines per branch, respectively. To elaborate the impact of the novel topology more precisely, the best performing oligomers containing the Stp and Sph building block were used for the comparison of the comb and their linear counterparts in regard to physical properties, cellular uptake, and plasmid DNA (pDNA) transfection efficiency.

EXPERIMENTAL PROCEDURES

Materials. Trityl OH-ChemMatrix resin was obtained from Biotage (Uppsala, Sweden). 1-Hydroxybenzotriazol (HOBt), triisopropylsilane (TIS), Triton X-100, hydrazine monohydrate, 2,2,2-trifluoroethanol (TFE), *N*-ethylmorpholine (NEM), and 3-(4,5-dimethylthiazol-2-yl)-2,5-diphenyltetrazolium bromide (MTT), diethylene triamine (DETA), triethylene tetramine (TETA), tetraethylene pentamine (TEPA), and pentaethylene hexamine (PEHA) were purchased from Sigma-Aldrich (Munich, Germany); benzotriazol-1-yl-oxy-tris-pyrrolidino-phosphonium hexafluorophosphate (PyBOP), 2-(1*H*-benzotriazole-1-yl)-1,1,3,3-tetramethyluronium hexafluorophosphate (HBTU), and microreactors for manual and automatic synthesis from MultiSynTech (Witten, Germany). Linear PEI (LPEI, 22 kDa average molecular weight) was synthesized as described.[28] All amino acids, peptide grade dimethylformamide (DMF), peptide grade *N*-methylpyrrolidone (NMP), diisopropyl-ethylamine (DIPEA), and trifluoroacetic acid (TFA) were purchased from Iris Biotech (Marktredwitz, Germany). The cationic building blocks Stp(boc)$_3$-Fmoc and Sph(boc)$_4$-Fmoc were synthesized as described,[14,20] respectively. Further, Boc-protected building blocks (Sdt(boc)$_2$−OH, Stt(boc)$_3$−OH, Stp(boc)$_4$−OH, and Sph(boc)$_5$−OH) were synthesized as described in the Supporting Information. Cell culture media, antibiotics, and fetal calf serum (FCS) were purchased from Invitrogen (Karlsruhe, Germany). Plasmid pCMVLuc was produced with the Qiagen Plasmid Giga Kit (Qiagen, Hilden, Germany) according to the manufacturer protocol. Cy5-labeling kit for pDNA labeling was obtained from Mirus Bio (Madison, WI, USA).

Methods. *General Procedure for Syntheses of Oligo(ethanamino)amide Carriers.* Oligomers were synthesized by standard protocols for solid phase peptide synthesis applying the Fmoc/tBu protecting group strategy analogously as described.[14,16] As solid support, 2-chlorotrityl chloride or trityl-ChemMatrix resins were used. The loading of resins is described in the Supporting Information. All structures were synthesized in a 7 μmol scale using a 2 mL syringe reactor. For manual synthesis, the resin was preswollen 20 min in DCM; for automatic synthesis, 20 min in NMP.

Comb Structure Synthesis. Two different strategies, a convergent manual and an automated synthesis, were tested. Suitability of both methods is shown in Figure S1 in the Supporting Information. The less time-consuming automated synthesis was preferentially used. The convergent manual strategy is described in the Supporting Information.

Comb Structures with Automated Synthesis. The automated microwave peptide synthesis was performed on the Syrowave system from Biotage AB (Uppsala, Sweden). The backbone was assembled on a ChemMatrix-Trityl-Fmoc-Cys-Trt resin with a loading of around 0.28 mmol/g preswollen in NMP for 20 min. N$^{\alpha}$-Fmoc deprotection was performed at 50 °C two times for 3 min with 40% piperidine in DMF, followed by 5 and 10 min with 20% piperidine in DMF. Amino acids (4 equiv, 0.23 M) were dissolved in 0.23 M HOBt in NMP, DIPEA (8 equiv) was dissolved in NMP, and HBTU (4 equiv) was dissolved in DMF. Double couplings were performed for 8 min at 75 °C. After each deprotection and coupling step the resin was washed 3 times with DMF. For backbone assembly Fmoc-Lys(Dde)-OH was used as well as Boc-Cys(Trt) in the last coupling step. For the backbones containing a spacer, amino acid Fmoc-Ala-OH or Fmoc-His(Trt)-OH were coupled after every lysine. After the backbone assembly the Dde-protecting group was removed by washing the resin with 2% hydrazine in DMF for 5 min and the absorbance of the cleavage solution was checked at 290 nm. The washing was repeated until the value of absorbance was below 0.1.

Linear Structures with Automated Synthesis. The automated microwave peptide synthesis was performed on the Syrowave system (Biotage AB). The sequences were assembled on a ChemMatrix-Trityl-Fmoc-Cys(Trt) resin with a loading of around 0.28 mmol/g preswollen in NMP for 20 min. N$^{\alpha}$-Fmoc deprotection was performed at 50 °C two times for 3 min with 40% piperidine in DMF, followed by 5 and 10 min with 20% piperidine in DMF. Amino acids (4 equiv, 0.23 M) were dissolved in 0.23 M HOBt in NMP, DIPEA (8 equiv) was dissolved in NMP, and HBTU (4 equiv) was dissolved in DMF. Double couplings were performed for 8 min at 75 °C. After each deprotection and coupling step the resin was washed 3 times with DMF. For backbone assembly, Fmoc-Lys(Boc)-OH was used alternating with the spacer amino acids Fmoc-Ala-OH or Fmoc-His(Trt)-OH as well as Boc-Cys(Trt) in the last coupling step.

Cleavage of the Oligomers. To cleave the peptides from the resin, it was treated with a cleavage solution containing TFA/TIS/H_2O (95:2.5:2.5) for 1.5 h. Afterward, the resin was washed twice with TFA and twice with DCM. All the solutions were combined, concentrated, and precipitated by dropwise addition into a mixture of *n*-hexane and MTBE (1:1) cooled to −20 °C. The pellet after centrifugation is dried under nitrogen and dissolved in the buffer for size exclusion consisting of 10 mM HCl and 30% acetonitrile. After purification by size exclusion on a G-10 column, the product-containing fractions were combined, frozen in liquid nitrogen, and lyophilized.

Polyplex Formation. Polyplexes were prepared by dissolving 200 ng of pDNA and oligomers at indicated nitrogen/phosphate (N/P) ratios each in a total volume of 10 μL HBG buffer. The polycation solution was added to the nucleic acid, rapidly mixed, and incubated for 30−40 min at RT.

pDNA Condensation − EtBr Exclusion Assay. DNA condensation ability was tested in the ethidium bromide (EtBr) exclusion assay. The effect of stepwise addition of polymer solution to 10 μg pDNA in 1 mL HBG containing 0.4 μg EtBr was measured at increasing N/P ratios using a Cary Eclipse spectrophotometer (Varian, Germany). Maximal fluorescence intensity was set to 100% for the EtBr solution containing free nucleic acid, and fluorescence decrease was measured 0.5 min after each addition of polymer aliquot.

DLS Measurement − Particle Size and Zeta Potential. Particle size and zeta potential of polyplexes were measured by laser-light scattering using a Zetasizer Nano ZS (Malvern Instruments, Worcestershire, U.K.). Five micrograms of pDNA was used for polyplex formation in 500 μL HEPES (pH 7.4). Before measurement, 400 μL HEPES was added.

a)

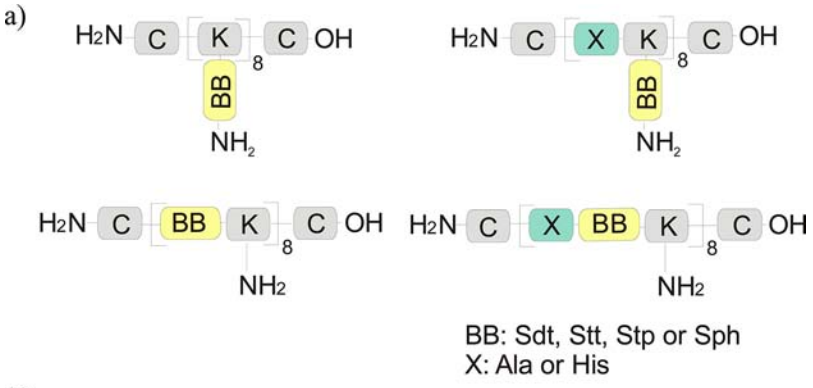

b)

	Building block (BB)	Prot N	Structure
Sdt	Succinyl-diethylene triamine	2	
Stt	Succinyl-triethylene tetramine	3	
Stp	Succinyl-tetraethylene pentamine	4	
Sph	Succinyl-pentaethylene hexamine	5	

Figure 1. Sequence-defined oligomers with comb or linear topology. (a) Schematic overview of the comb and linear carrier structures used with and without different spacer molecules (X: Ala or His). (b) Structure of the artificial amino acids Sdt, Stt, Stp, and Sph that were incorporated into comb or linear structures. Prot N = number of protonatable amines.

Buffer Capacity – pH Titrations. The oligomer sample, containing 15 μmol protonatable amines, was diluted in a total volume of 3.5 mL NaCl solution (50 mM) and the pH was adjusted to 2.1 by addition of 0.1 M hydrochloric acid. Afterward, a back-titration with 0.05 M NaOH solution was performed with an automatic titration system (Titrando 905 from Metrohm, Germany) until pH of 11 was reached. Furthermore, a titration with 50 mM NaCl was performed and the consumption of NaOH in this control titration was subtracted from the consumption in the oligomer titrations at the corresponding pH values. Percentage of buffer capacity C in a certain pH range (x–y), where ΔV stands for the volume consumption of NaOH in the considered pH range, was calculated according to the following equation:

$$C_{\mathrm{pH}x-y} = \frac{\Delta V_{\mathrm{pH}x-y} \times 0.05\ \mathrm{M}}{0.015\ \mathrm{mmol}} \times 100$$

Cell Culture. Mouse neuroblastoma cells Neuro2A were grown in Dulbecco's modified Eagle's medium (DMEM), supplemented with 10% FCS, 4 mM stable glutamine, 100 U/mL penicillin, and 100 μg/mL streptomycin.

Cellular Association and Internalization by Flow Cytometry. Neuro2A cells were seeded into 24-well plates coated with collagen at a density of 50 000 cells per well. After 24 h, culture medium was replaced with 400 μL fresh growth medium. Polyplexes prepared at N/P 12 in 100 μL HBG, containing 1 μg pDNA (20% of the nucleic acid was Cy5-labeled) were added to each well and incubated either at 37 °C for internalization, or at 0 °C for association studies for 1 or 4 h. All experiments were performed in triplicate. Subsequently, only for measurement of internalization, to remove polyplexes on the cell surface, cells were washed for 15 min with 500 μL PBS, containing 1000 IU of heparin. Cells were detached with trypsin/EDTA and taken up in PBS with 10% FCS. Cellular uptake was assayed by excitation of Cy5 at 635 nm and detection of emission at 665 nm. Cells were appropriately gated by forward/sideward scatter and pulse width for exclusion of doublets. DAPI (4′,6-diamidino-2-phenylindole) was used to discriminate between viable and dead cells. Data were recorded by Cyan ADP flow Cytometer (Dako, Hamburg, Germany) using Summit acquisition software (Summit, Jamesville, NY, USA) and analyzed by FlowJo 7.6.5 flow cytometric analysis software.

Gene Transfer – Luciferase Assay. Neuro2A cells were seeded in 96-well plates 24 h prior to transfections using 10 000 cells per well. Polyplexes were formed in 20 μL HBG with 200 ng pCMVLuc encoding plasmid per well and the calculated amount of polymer corresponding to the N/P ratio. All experiments were performed in quintuplicate. Before transfection, medium was replaced with 80 μL fresh medium containing 10% FCS. Twenty-four hours after transfection, cells were treated with 100 μL cell lysis buffer (25 mM Tris, pH 7.8,

dx.doi.org/10.1021/bc400392y | *Bioconjugate Chem.* 2014, 25, 251–261

Table 1. Sequences of Comb and Linear Structures Written from N- to C-Terminus and the Corresponding Codes Used Throughout the Text[a]

building block	compound ID	sequence	code	protonatable amines
Sdt comb (2 prot N)	632	C-[K(Sdt)]$_8$-C	Sdt-cmb-0	17
	633	C-[A-K(Sdt)]$_8$-C	Sdt-cmb-A	17
	634	C-[H-K(Sdt)]$_8$-C	Sdt-cmb-H	17
Stt comb (3 prot N)	635	C-[K(Stt)]$_8$-C	Stt-cmb-0	25
	636	C-[A-K(Stt)]$_8$-C	Stt-cmb-A	25
	637	C-[H-K(Stt)]$_8$-C	Stt-cmb-H	25
Stp comb (4 prot N)	622	C-[K(Stp)]$_8$-C	Stp-cmb-0	33
	551	C-[A-K(Stp)]$_8$-C	Stp-cmb-A	33
	552	C-[H-K(Stp)]$_8$-C	Stp-cmb-H	33
Sph comb (5 prot N)	629	C-[K(Sph)]$_8$-C	Sph-cmb-0	41
	630	C-[A-K(Sph)]$_8$-C	Sph-cmb-A	41
	631	C-[H-K(Sph)]$_8$-C	Sph-cmb-H	41
Stp linear (3 prot N)	625	C-(Stp-K)$_8$-C	Stp-lin-0	33
	626	C-(A-Stp-K)$_8$-C	Stp-lin-A	33
	628	C-(H-Stp-K)$_8$-C	Stp-lin-H	33
Sph linear (4 prot N)	648	C-(Sph-K)$_8$-C	Sph-lin-0	41
	649	C-(A-Sph-K)$_8$-C	Sph-lin-A	41
	650	C-(H-Sph-K)$_8$-C	Sph-lin-H	41

[a]Cmb = comb. lin = linear. 0 = no spacer amino acid. A = alanine spacer. H = histidine spacer. prot N = number of protonatable nitrogens per building block.

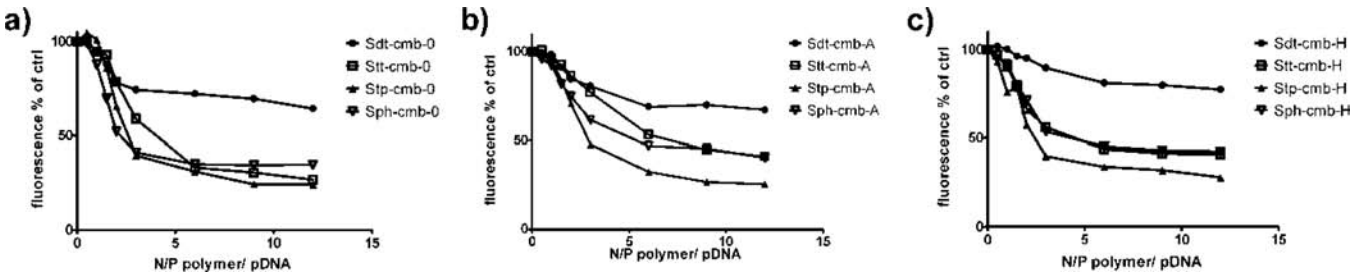

Figure 2. pDNA binding capacity of comb-type oligomers. EtBr exclusion assays of Sdt, Stt, Stp, and Sph comb structures with increasing N/P ratios obtained by stepwise addition of the oligomer to pDNA solution at pH 7.4. 100% value displays fluorescence intensity of DNA and EtBr before the addition of the polymer: (a) without spacer, (b) Ala spacer, (c) His spacer.

2 mM EDTA, 2 mM DTT, 10% glycerol, 1% Triton X-100). Luciferase activity in the cell lysate was measured using a luciferase assay kit (100 μL Luciferase Assay buffer, Promega, Mannheim, Germany) and a Lumat LB9507 luminometer (Berthold, Bad Wildbad, Germany).

RESULTS

Comparison of Comb Structures with Different Number of Ethylene Amine Repeating Units. *Carrier Synthesis and Design.* The solid-phase assisted synthesis of cationic oligomers using the artificial oligoamino acids Stp or Sph has been used to establish polymer libraries including effective carriers for gene delivery.[15,16,20] In these previous studies the artificial amino acids were incorporated into the oligomer backbone. Here we present new comb-like structures. Four different building blocks, Sdt, Stt, Stp, and Sph, with differing numbers of amino ethylene units, were attached to an oligolysine backbone, resulting in formation of eight oligoamine branches (Figure 1). Because the terminal amines remain free instead of being part of the subsequent amide bond as for the linear shaped oligomers, in these comb oligomers each artificial amino acid provides one additional protonatable amine. Furthermore, terminal cysteines were included in the comb structures because the disulfide formation during polyplex formation has been shown to be important for stabilization and thus transfection efficiency.[15,20] This benefit could also been demonstrated for the comb structures, as a cysteine containing structure showed better DNA binding compared to the analogous alanine-containing control sequence. The strong binding was weakened by treatment with the reducing agent TCEP, whereas no effect of TCEP could be observed for the alanine control oligomer (Figure S2). Initial studies of comb structures with 4 repeating lysine units had shown only low pDNA transfection efficiency (Figure S3). Increasing the number to 8 branches improved the biological performance so that this number was chosen for the design of all subsequent comb structures. To vary the distance between the comb branches, different natural amino acids were incorporated in the oligolysine backbone (Figure 1a). Alanine was used to evaluate the effect of a spacer between the branches. Alternatively, histidine was included, which had been shown to improve the buffer capacity at endosomal pH and the transfection efficiency for carriers.[29] A list of all synthesized structures is presented in Table 1.

Biophysical Properties. Next, we tested the pDNA binding characteristics of the comb oligomers. The agarose gel shift assay demonstrated complete pDNA complexation ability at N/P ratio of 6 and higher for all oligomers with Stt, Stp, and Sph

dx.doi.org/10.1021/bc400392y | Bioconjugate Chem. 2014, 25, 251−261

building block (Figure S4a). The Sdt oligomers with only two protonatable amines per comb unit showed the weakest binding which was complete only at N/P 12 and higher. As exception, the histidine containing Sdt structures showed complete binding already at N/P 3. These findings were verified in the EtBr exclusion assay, where the Sdt oligomers showed the lowest fluorescence decrease independent of the spacer (Figure 2). Stt and Sph oligomers compacted the pDNA to a similar extent, while for the Stp sequences an enhanced pDNA condensation ability could be observed. This was less pronounced for the structures without spacer molecule.

Particle sizes measured with DLS greatly differed depending on the length of the ethylene amine building block (Table 2a).

Table 2. Particle Size (indicated as *Z*-average). Polydispersity Index (PDI). and Zeta Potential of pDNA Complexes with (a) Comb Oligomers and (b) Linear Oligomers at N/P 12 Measured by DLS

	Z-average [nm]	PDI	zeta potential [mV]
	(a)		
Sdt-cmb-0	2128.7 ± 147.7	0.861	14.5 ± 0.3
Sdt-cmb-A	607.7 ± 18.7	0.394	17.9 ± 0.2
Sdt-cmb-H	444.0 ± 35.3	0.353	16.2 ± 0.6
Stt-cmb-0	175.3 ± 12.9	0.291	10.0 ± 0.8
Stt-cmb-A	259.3 ± 3.7	0.184	4.2 ± 0.1
Stt-cmb-H	255.6 ± 23.2	0.277	12.8 ± 1.2
Stp-cmb-0	136.4 ± 4.0	0.354	27.8 ± 0.1
Stp-cmb-A	103.6 ± 8.7	0.309	34.2 ± 0.5
Stp-cmb-H	102.5 ± 9.8	0.319	28.9 ± 0.5
Sph-cmb-0	109.5 ± 5.4	0.138	26.0 ± 0.1
Sph-cmb-A	132.3 ± 3.5	0.244	23.8 ± 0.7
Sph-cmb-H	167.3 ± 17.6	0.371	18.3 ± 1.5
	(b)		
Stp-lin-0	112.9 ± 12.9	0.359	26.2 ± 0.8
Stp-lin-A	85.8 ± 3.9	0.226	26.0 ± 0.4
Stp-lin-H	131.6 ± 3.6	0.314	28.7 ± 0.4
Sph-lin-0	117.4 ± 12.2	0.195	14.6 ± 3.7
Sph-lin-A	127.9 ± 4.0	0.276	12.4 ± 0.6
Sph-lin-H	125.3 ± 3.4	0.313	21.8 ± 0.3

Oligomers consisting of the shortest, less protonated building block formed the biggest particles. Sdt oligomers without spacer formed aggregates of about 2 μm. Sdt oligomers with Ala and His spacer formed particles of about 600 and 400 nm, which are still more than 3- and 2-fold bigger than particles formed with structures containing the other building blocks of increasing length. With sizes between 170 and 260 nm also the Stt oligomers produced particles clearly bigger than the Stp and Sph oligomers. For Stp oligomers the smallest particles in a range between 100 and 140 nm were observed. They display the highest zeta potential between 27 and 35 mV. Overall, we observed a tendency of decreasing particle size with increasing number of ethylene amine units.

The buffer capacity of the oligomers (Figure 3) was measured by alkalimetric titration in the pH range between 5.0 and 7.4. Figure 3b-d shows the differential buffer capacities within this pH range; Figure 3a shows the sum of differential buffer capacities presented as the total buffer capacity between pH 5.0 and 7.4. This range represents the physiologically relevant acidification from pH 7.4 in the extracellular compartment to pH 5.5 in the endosome. Clear differences in the buffer capacity could be found for the comb structures with increasing number of protonatable amines. The Sdt oligomers with only two protonatable amines per branch exhibited by far the highest buffering capacity (Figure 3a). Stt oligomers with three protonatable amines per branch displayed the lowest buffering capacity for the structures without spacer and Ala spacer. Increasing the number to four protonatable amines led to an increase in the total buffer capacity between pH 5.0 and 7.4, whereas a further extension to five protonatable amines per branch, which can be found in the Sph structures, resulted in a small decrease in the buffer capacity. Regardless of the building block, the histidine containing oligomers showed the highest total buffer capacity in the pH range between 5.0 and 7.4.

On closer examination of the differential buffer capacity in the relevant pH range, two different buffering profiles are revealed (Figure 3b-d). Sdt and Stp containing oligomers with 2 and 4 protonatable amines per branch have the maximum buffer capacity between pH 5.5 and 6.5, while Stt and Sph sequences with 3 or 5 protonatable amines in a row exhibit their maximum capacity between 6.5 and 7.4 (Figure 3b,c). Only for the histidine containing structures are discrepancies from this trend observed. This is predictable due to an additive buffering effect of histidine around the pH of 6 (Figure 3d).

Cellular Uptake and Gene Transfer. As an initial measure of the biological efficiency, the cellular uptake of the comb oligomers with different length of amino ethylene building blocks was investigated in Neuro2A cells by incubation of the cells at 37 °C with polyplexes formed at N/P 12 and containing 20% of Cy5-labeled DNA (Figure S5). The incubation time of 4 h was followed by a heparin washing step in order to remove polyplexes attached on the cell surfaces. Polyplexes formed with Stt, Stp, and Sph oligomers displayed a similar uptake rate independent of the spacer. In the case of the Sdt oligomers without spacer the polyplexes were not internalized by the cells. For the Ala- and His-containing Sdt structures only a small subpopulation of cells did not internalize any particles. The greater fraction of cells showed similar fluorescence intensities as observed for the Stt, Stp, and Sph oligomers in the flow cytometric analysis.

Initial testings of luciferase pDNA transfection efficiency, which was determined 24 h after polyplex addition in Neuro2A cells, revealed that the Stp-containing comb structures modulate the highest gene transfer among the tested building blocks (Figure S6). Histidine containing oligomers displayed the greatest gene transfer efficiency in each group. Except for the Stt oligomers, the Ala spacer also resulted in a higher gene expression compared to the structures without spacer. The best performing sequence, Stp-cmb-H, at the N/P ratio of 6 exceeded LPEI 26-fold at its most effective, nontoxic concentration (Figure S7).

To examine cytotoxicity, MTT assays were performed at different N/P ratios in parallel to the luciferase assay in Neuro2A cells. The metabolic activity values yielded between 80% and 110% after pDNA transfection (Figure S8a) indicating that none of the oligomers displayed severe toxicity under the tested conditions.

Comparison of the Different Topologies of Comb versus Linear Shaped Oligomers. *Carrier Synthesis and Design.* The primary results already revealed that the comb-like structure may provide effective carriers for pDNA delivery. In the following, the most promising sequences, which were those bearing Stp or Sph branches, were compared to corresponding linear structures containing the identical type and number of

dx.doi.org/10.1021/bc400392y | *Bioconjugate Chem.* 2014, 25, 251−261

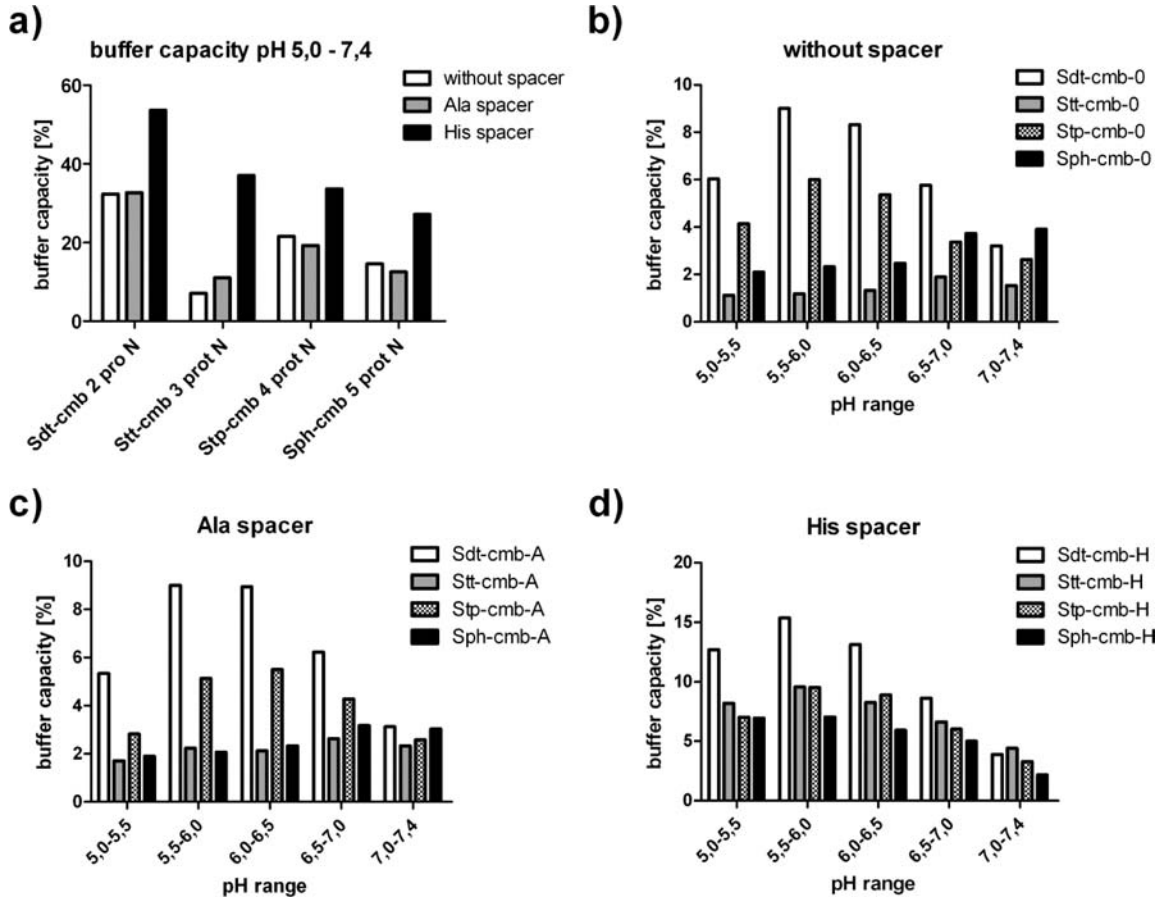

Figure 3. Buffer capacity of comb-type oligomers. (a) Total buffer capacity of Sdt, Stt, Stp, and Sph comb structures measured in the pH range of 5.0−7.4. (b)−(d) Differential buffer capacities between pH 5.0 and 7.4: (b) without spacer, (c) with Ala spacer, and (d) with His spacer.

amino acids, but with the Stp or Sph building blocks attached to the α-amino group of lysine instead of the corresponding ε-amino group of the oligomer backbone. Therefore, the total number of protonatable amines remains the same in both carrier types, but the length of oligomer backbone strongly differs. The synthesis of the linear control sequences (Table 1) was performed on an automated peptide synthesizer as described in the Supporting Information.

Biophysical Properties. The pDNA complexation ability of the branched and linear oligomers was examined at different N/P ratios using the agarose gel shift assay. All the comb and linear oligomers showed partial DNA binding at N/P 3 and complete binding at N/P 6 and higher (Figure S3). To investigate the influence of the N/P ratio on the binding capability in more detail, an EtBr exclusion assay was performed increasing the N/P ratio in steps of 0.5 from N/P 0 to 2 and bigger steps up to N/P 12 (Figure S9). Except for the Stp containing structures with Ala spacer, all linear structures showed a better DNA condensation ability compared to the corresponding comb structures. This effect was less pronounced for the structures with histidine spacer (Stp-lin-H vs Stp-cmb-H). The results are in agreement with the data obtained in the gel shift assay and demonstrate an advantageous DNA binding for the linear structures. However, both comb- and linear-type structures are able to form stable polyplexes with pDNA at N/P ratios higher than 5.

We next determined the particle size and zeta potential of oligomer/pDNA complexes at N/P 12 by DLS (Table 2). The mean sizes of the polyplexes of the Stp comb type structures were about 100 to 130 nm. Polyplex sizes were quite similar for the linear structures with a range between 85 and 135 nm. For Sph-containing structures slightly bigger sizes were observed, in the range of 100 to 170 nm for the comb structures and 115 to 130 nm for the linear structures, but revealing again no significantly differing effect of the topology on the polyplex size. Independent of the building block, the zeta potential of comb structures without spacer or Ala spacer displayed a slightly higher zeta potential than the corresponding linear structure. The zeta potential was quite similar for His containing structures (Table 2).

By comparison of the differential buffer capacities between pH 5.0 and 7.4 in detail, a clear difference in the buffering profiles became obvious (Figure 4). For Stp oligomers with four protonatable amines in the comb type and three in the linear type, all comb structures displayed the highest buffer capacity between pH 5.0 and 6.5, whereas the maximum buffer capacity of the linear oligomers was observed between pH 6.5 and 7.4 (Figure 4a,b). An opposite effect could be observed for the Sph oligomers, where four protonatable amines are provided in the linear structures and five in the comb structures. Here the linear oligomers demonstrated a clearly higher buffer capacity between pH 5.0 and 6.5, whereas the highest buffer capacity of the comb oligomers was observed between pH 6.5 and 7.4 (Figure 4d,e). As histidine enhances the buffer capacity at pH 6, an additive effect at this pH could be observed for the histidine-containing oligomers, so that the already high buffer capacity at this pH was further increased for the Stp comb and Sph linear structures, whereas the Stp linear

dx.doi.org/10.1021/bc400392y | *Bioconjugate Chem.* 2014, 25, 251−261

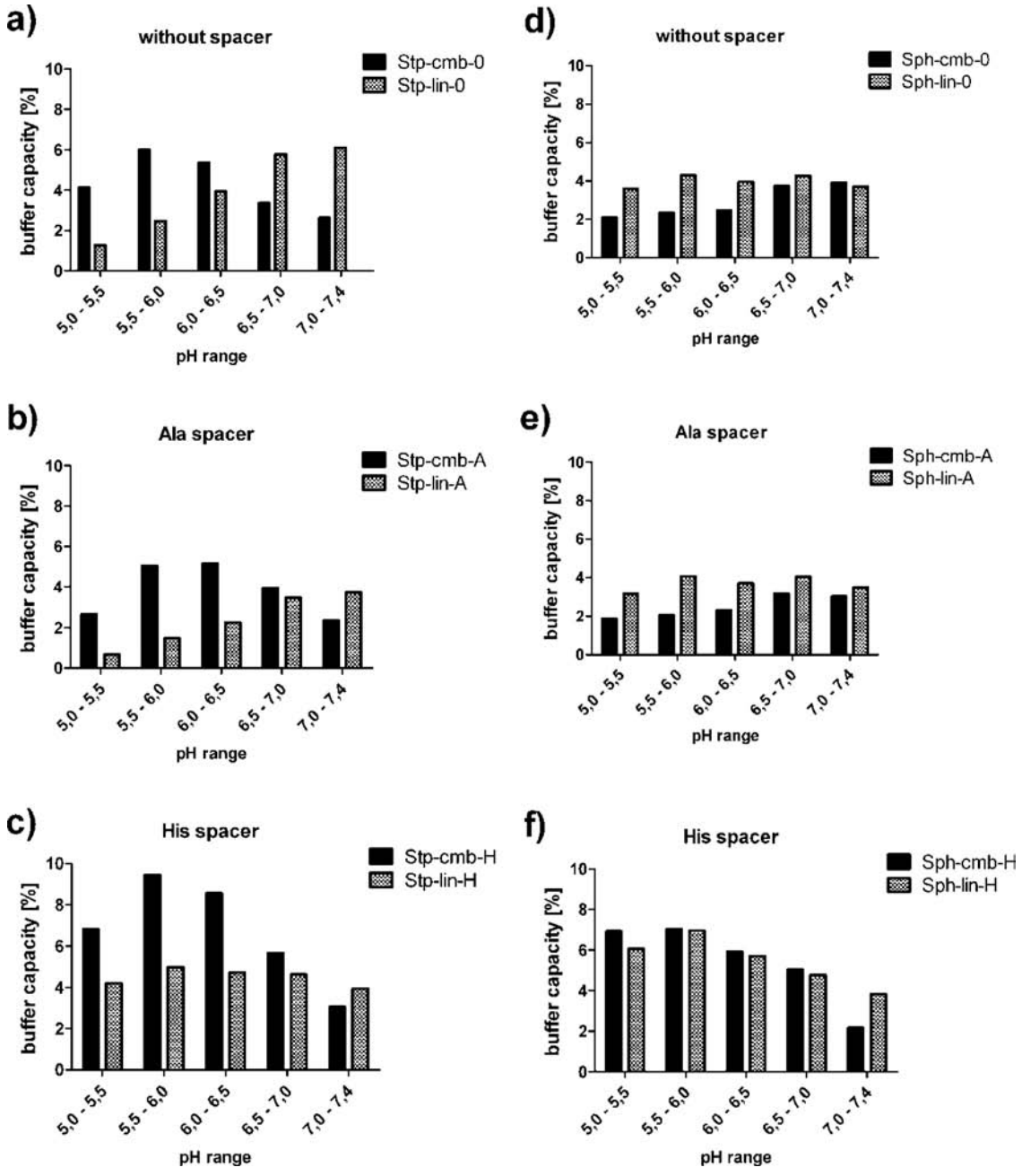

Figure 4. Comparison of differential buffer capacities of Stp- and Sph-based comb and linear structures between pH 5.0 and 7.4. (a) Stp oligomers without spacer, (b) Stp oligomers with Ala spacer, (c) Stp oligomers with His spacer, (d) Sph oligomers without spacer, (e) Sph oligomers with Ala spacer, (f) Sph oligomers with His spacer.

and Sph comb structures consequently showed a broader buffer capacity over the whole pH range from 5.0 to 7.4 (Figure 4c,f).

Cellular Association, Intracellular Uptake, and Gene Transfer. To compare the biological efficiency of the Stp and Sph comb and linear oligomers, the cellular association of polyplexes at N/P 12 was investigated in Neuro2A cells (Figure 5a,b). After one hour at 0 °C, the linear structures displayed a higher amount of polyplexes bound to the cells. After four hours of incubation, the cellular association was similar for comb and linear structures (Figure S10a,b).

Next, the intracellular uptake of polyplexes was investigated after four hours at 37 °C with a subsequent heparin washing step to remove polyplexes from the cell surfaces (Figure 5c,d). Interestingly and independent of the ethylene amine building block and the spacer amino acid, the comb type structures displayed higher intracellular uptake rates than their linear counterparts. Cellular uptake was already higher for the comb structures than the linear structures after one hour (Figure S10c,d) and approximately 3- to 4-fold higher for the Stp combs (Figure 5c) and 5- to 11-fold higher for the Sph combs (Figure 5d) after four hours.

The reasons for the discrepancy between cell association and intracellular uptake, and the differing effect of oligomer topology, remain unclear. Simple biophysical properties such as zeta potential can be ruled out as dominating parameters. In the case of Stp-cmb-A, Sph-cmb-0, and Sph-cmb-A the zeta potential of the comb structures was higher than for the linear structures, which correlates with their enhanced cellular

dx.doi.org/10.1021/bc400392y | *Bioconjugate Chem.* 2014, 25, 251−261

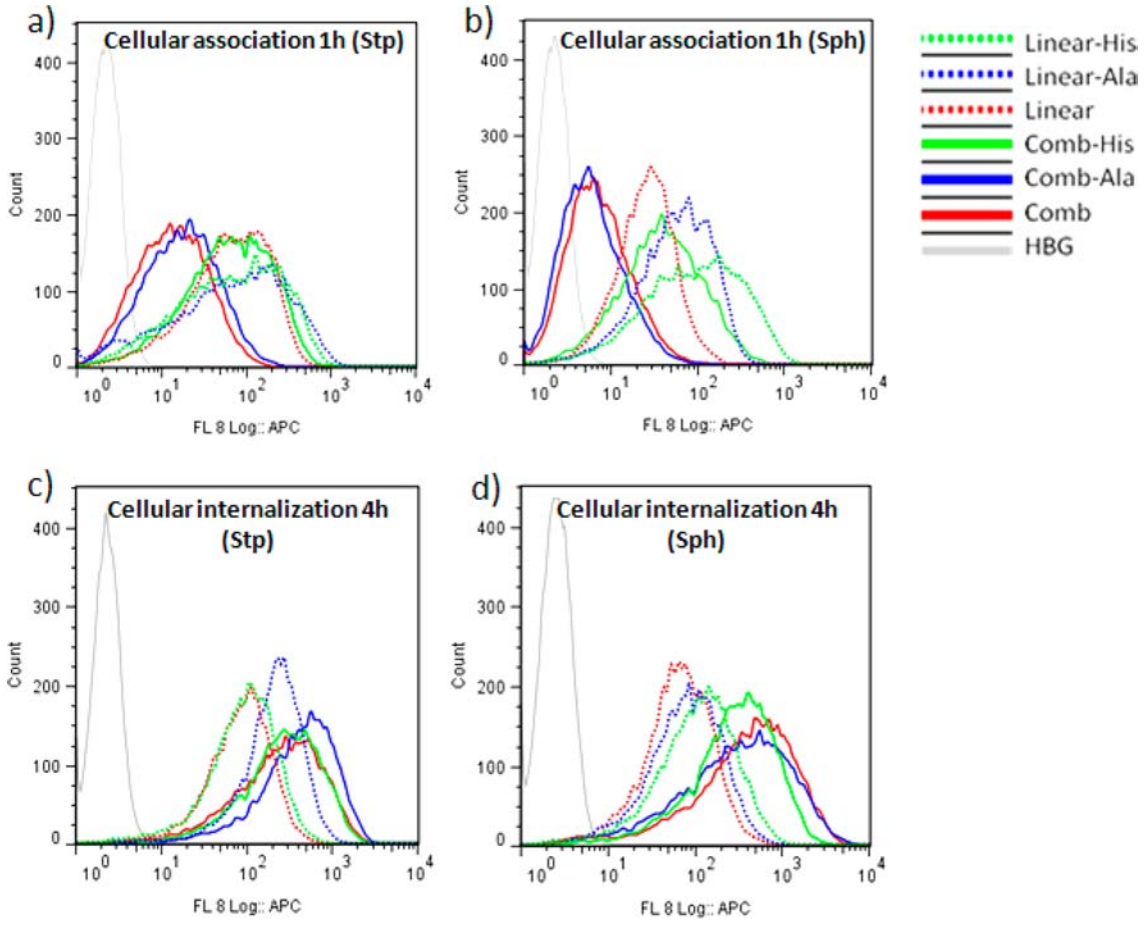

Figure 5. Cell binding and intracellular uptake of polyplexes. (a,b) Cellular association of Cy5-labeled pDNA/oligomer complexes at N/P 12 with (a) Stp and (b) Sph determined by flow cytometry in Neuro2A cells after 1 h on ice. (c,d) Cellular internalization of Cy5-labeled DNA/oligomer complexes at N/P 12 with (c) Stp and (d) Sph determined by flow cytometry in Neuro2A cells after 4 h at 37 °C. Comb structures are displayed with solid lines, linear structures with dotted lines. Without spacer = red, Ala spacer = blue, and His spacer = green. *X*-axis represents the intensity of the Cy5 signal and "Count" the number of cell counts with according fluorescence signal after appropriate gating. All incubations were performed in standard serum-supplemented culture medium. In the internalization studies, cells were washed for 15 min with heparin to remove polyplexes on the cell surface (see Materials and Methods).

internalization. However, for the other examined structure pairs the measured zeta potential was similar but the enhanced uptake was still observed. To evaluate the option that the different fluorescence intensities measured in the flow cytometry experiments might result from different quenching effects of comb and linear structures, the fluorescence of polyplexes of oligomers of both topologies with the same amounts of DNA were determined and compared to the signal of the same amount of free DNA. Although the quenching of the linear structures was around 2-fold higher than for the comb structures (Figure S11) this cannot account for the clearly (up to 11-fold) enhanced uptake of the comb structure polyplexes observed in flow cytometry. Moreover, the higher fluorescence of polyplexes of linear structures in the cell association studies is opposite to the slightly higher fluorescence quenching, suggesting that the cell binding difference might even be more pronounced than displayed by the comparison of fluorescence.

The polymers were compared in their pDNA transfection efficiency (Figure 6). For Stp oligomers, the gene transfer levels of the comb type oligomers were 7- to up to 340-fold higher compared to the linear structures (Figure 6a). The histidine containing oligomers displayed the greatest gene transfer efficiency. Evaluation of the pDNA transfection efficiency of Sph comb and linear structures also revealed some higher gene transfer efficiency of the comb type oligomers, but compared to the Stp oligomers this effect was less pronounced (Figure 6b).

MTT assay was performed at different N/P ratios with mean values of around 100% metabolic activity for Stp sequences and values above 80% for Sph sequences (Figure S8) displaying no severe cytotoxicity under the tested conditions.

■ DISCUSSION

Gene delivery is a promising tool for medical treatment, but several bottlenecks need to be overcome in order to successfully deliver pDNA into the target cells and achieve gene expression. Therefore, the usage of appropriate carrier systems with specific properties is an essential task. Solid-phase assisted peptide synthesis offers the opportunity to design sequence-defined cationic carriers for this purpose. Based on the knowledge of structure−activity relationships of an already existing library of sequence-defined cationic carriers for pDNA delivery,[16] in this study new comb-like structures were designed and synthesized by attaching the four artificial amino acids, Sdt, Stt, Stp, and Sph (differing in the numbers of cationizable nitrogens from two to five), to an oligolysine backbone (Figure

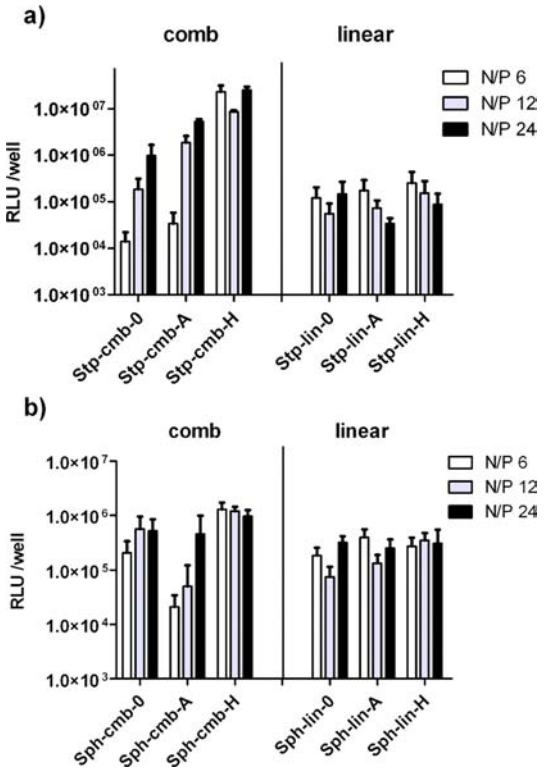

Figure 6. Luciferase gene transfer by comb versus linear carriers. (a) Stp and (b) Sph oligomers tested with pCMVLuc pDNA in Neuro2A cells at N/P ratios 6, 12, and 24.

1). Terminal cysteines were incorporated for a beneficial stabilization of polyplexes by means of disulfide formation as previously reported for linear structures.[15,16,20] We compared the biophysical properties of the oligomers and their performance in biological application. Out of the tested building blocks, Stp and Sph were found to be the most suitable ones for synthesizing effective comb structures for pDNA delivery. Therefore, these comb structures were subsequently compared to the corresponding linear control sequences to specifically investigate the influence of the topology. We demonstrate that the carrier topology had significant influence on the properties of the oligomers.

In analysis of comb oligomers with the different oligoamino acid building blocks, the ability of DNA complexation was investigated by EtBr assay. The weakest DNA binding was revealed for Sdt oligomers, indicating that these structures are the least suited among the tested compounds. Consistent with the weak DNA binding, pH titrations revealed a less protonated state at pH 7.4 and therefore potentially less electrostatic interactions with the negatively charged DNA. Sdt structures were not able to form small and stable particles. The formation of big aggregates of around 2 μm for Sdt-cmb-0 may account for the very low cellular uptake. Also, polyplexes with Sdt-cmb-A and Sdt-cmb-H displayed larger particle sizes and only a small fraction of particles internalized to the cells. Nevertheless, some transfection efficiency was observed for the Sdt oligomers in the luciferase assay. A possible reason might be an improved endosomal release based on effective endosomal buffering and protonation. Sdt comb oligomers display the highest buffer capacity between pH 5.0 and 7.4 among the tested oligomers. In contrast, Stt oligomers showed the worst buffering capacity. The particle sizes were around 2-fold higher compared to the polyplexes formed with the Stp structures. The latter ones resulted in the smallest particles with the highest positive zeta potential. Together with the high buffering capacity the beneficial nanoparticle characteristics mark the Stp comb structures as potent carriers for gene delivery.

To investigate which properties can be attributed to the specific comb topology, linear control Stp sequences were synthesized and directly compared in terms of biophysical properties and biological performance. To further explore to which extent the different behavior is a consequence of the topology or an effect of the variation of the protonatable ethylene amine building block length, the same comparison was performed with the Sph containing comb and linear structures.

Superior pDNA binding of the histidine-free linear structures was displayed by the EtBr assay, whereas for the histidine-containing structures a similar pDNA condensation ability of linear and comb structures could be observed, in the case of both Stp and Sph based oligomers. A possible explanation is that histidine also contributes to the pDNA complexation ability and polyplex stabilization of these structures, therefore mitigating the difference in performance of comb and linear type. Furthermore, the tests revealed that at N/P 12 the DNA condensation was complete for all oligomers, so that this N/P ratio was used for further studies aimed at comparing particle size, zeta potential, cellular uptake, and association.

A most prominent distinction of comb and linear structures was found in the buffer capacity at the physiological relevant pH range between 5.0 and 7.4. Kataoka et al.[26] proposed the so-called "odd−even effect", reporting that polymers with side chains consisting of an even number of protonatable amino ethylene units provide high buffer capacity in this pH range and therefore a high transfection efficiency, while polymers with odd-numbered amino ethylene side chains display low buffer capacity and hence also low transfection efficiency. This assumption is based on the fact that changes in protonation from pH 7.4 to pH 5.0 occur for even-numbered structures, while electrostatic repulsion prohibits further protonation for odd-numbered structures, resulting in a lower buffer capacity. This model is confirmed in the current study by the comparison of the buffering capacity of Sdt, Stt, Stp, and Sph building blocks. Sdt and Stp containing comb structures with even-numbered protonatable amines show a higher buffer capacity than the odd-numbered Stt and Sph containing structures. Nevertheless, only partial accordance with the hypothetical model can be found in the comparison of comb and linear topology. Stp units in the comb sequences provide four protonatable amines (even number) and in the linear structures only three (odd number). Therefore the total buffer capacity should be higher for the comb structures, while in comparison of the Sph combs (five protonatable amines = odd number) with Sph linear structures (four protonatable amines = even number) the linear structures were expected to provide a higher total buffer capacity. The fact that free amines of the lysine in the linear structures result in the same total number of protonatable amines in both structure types shows that not the total number, but the intramolecular localization plays a crucial role. In both cases, comparing Stp and Sph comb and linear structures, we found a similar total buffer capacity between pH 5.0 and 7.4. However, a modified "odd−even rule" becomes apparent with regard to the buffering profile. The results clearly demonstrate that an odd number of protonatable amines in a row leads to a maximum buffer capacity in the pH range from 6.5 to 7.4 and an even number of protonatable amines results in

dx.doi.org/10.1021/bc400392y | Bioconjugate Chem. 2014, 25, 251−261

a maximum buffer capacity at pH 5.0 to 6.5. Especially, the higher buffer capacity from pH 5.0 to 6.5, which corresponds to the endosomal pH, may be contributing to an enhanced endosomal release. These findings give deeper insight into this phenomenon and contribute to understanding the superior performance in gene transfer of structures with higher buffering capacity at the relevant pH range.[26,29] Remarkably, for all types of carriers the histidine-containing sequences displayed the highest gene transfer consistent with the general notion that an increased buffer and protonation capacity at endosomal pH may enhance endosomal escape ('proton sponge effect') and gene transfer.[12,13,30−32] According to our results in terms of buffer capacity, the Stp building block is more beneficial when using it in the comb topology.

The comb and linear topology resulted in a further clear difference with regard to cellular association and internalization. In the cell association assay performed by incubation at 0 °C (to block internalization), after one hour the polyplexes formed with linear structures showed an increased cell association compared to the comb structures. After four hours the measured cell binding of polyplexes of comb and linear sequences was similar. Surprisingly, all Stp and Sph comb structures displayed an enhanced cellular uptake in comparison to their linear counterparts. This trend was observed already at one hour incubation time and clearly visible after four hours (Figure 4). As no remarkable differences could be observed for the sizes and zeta potential of comb and linear structures, these studies clearly demonstrate that the uptake process is considerably influenced by the carrier topology. Whether oligomer topology alters the nanoparticle surface exposed in cellular interaction, or whether the different free oligomers trigger cell uptake processes in a different manner, remains to be investigated. The fact that linear oligomers result in slightly higher fluorescence quenching in polyplexes containing Cy5-labeled DNA can only be a minor reason for the observed enhanced cellular fluorescence of the comb structure polyplexes in the flow cytometric cell uptake studies. Furthermore, the observations of different cellular uptake behavior are in agreement with other studies showing that nanoparticle shape and surface can influence the cellular uptake and binding on the cell surface.[33,34]

Interestingly, the different transfection efficiencies of oligomers without spacer or with Ala spacer indicate that not only may the total amount of cationic charges and buffering be important, but also the orientation and distance of the charged domains, which is changing the charge density and hence several biophysical properties.

CONCLUSIONS

In summary, this study reveals that a change in topology of sequence-defined oligoamino acid based pDNA carriers from linear to comb-like design results in a distinct change in buffer capacity profile of oligomers and intracellular uptake of corresponding pDNA polyplexes.

For the Sph oligomers the linear structures show an increased buffer capacity at endosomal pH, but the comb structures display a higher cellular uptake. These two opposing trends result in an only slightly higher transfection efficiency of the comb structures. For the Stp oligomers the comb structures mediate the preferred endosomal buffering profile and enhanced cellular uptake. This additive comb benefit contributes to a strongly enhanced efficacy of Stp combs for pDNA delivery.

ASSOCIATED CONTENT

Supporting Information

Additional supporting figures and data for synthetic procedures (resin loading, peptide synthesis, building block synthesis), analytical characterization (NMR, HPLC), further methods, and experimental data (agarose gel shift assay, DLS, MTT). This material is available free of charge via the Internet at http://pubs.acs.org.

AUTHOR INFORMATION

Corresponding Author

*Tel +49 89 2180 77841, Fax +49 89 2180 77798, E-mail: ernst.wagner@cup.uni-muenchen.de.

Notes

The authors declare no competing financial interest.

ACKNOWLEDGMENTS

This work was partly supported by the DFG Cluster "Nanosystems Initiative Munich", by a grant from Roche Kulmbach and the Biotech Cluster m4 project T12. We thank Naresh Badgujar for support in the building block synthesis, Olga Brück for assistance in preparing the manuscript, and Wolfgang Rödl for technical support.

ABBREVIATIONS

DAPI, 4′,6-diamidino-2-phenylindole; DCM, dichloromethane; DETA, diethylene triamine; DIPEA, diisopropyl-ethylamine; DLS, dynamic light scattering; DMEM, Dulbecco's modified Eagle's medium; DMF, dimethylformamide; DTT, dithiothreitol; EtBr, ethidium bromide; FCS, fetal calf serum; HBG, HEPES-buffered glucose; HBTU, 2-(1*H*-benzotriazole-1-yl)-1,1,3,3-tetramethyluronium hexafluorophosphate; HOBt, 1-hydroxybenzotriazol; LPEI, linear PEI; MTBE, *tert*-butyl methyl ether; MTT, (3-(4,5-dimethylthiazol-2-yl)-2,5-diphenyl-tetrazolium bromide); NEM, *N*-ethylmorpholine; NMP, *N*-methylpyrrolidone; PBS, phosphate-buffered saline; pDNA, plasmid DNA; PEHA, pentaethylene hexamine; PEI, polyethylenimine; PyBOP, benzotriazol-1-yl-oxy-tris-pyrrolidino-phosphonium hexafluorophosphate; RLU, relative light units; Sdt, succionyl-diethylene triamine; Sph, succionyl-pentaethylene hexamine; Stp, succionyl-tetraethylene pentamine; Stt, succionyl-triethylene tetramine; TEPA, tetraethylene pentamine; TETA, triethylene tetramine; TFA, trifluoroacetic acid; TFE, 2,2,2-trifluoroethanol; THF, tetrahydrofurane; TIS, triisopropylsilane

REFERENCES

(1) Boussif, O., Lezoualc'h, F., Zanta, M. A., Mergny, M. D., Scherman, D., Demeneix, B., and Behr, J. P. (1995) A versatile vector for gene and oligonucleotide transfer into cells in culture and in vivo: polyethylenimine. *Proc. Natl. Acad. Sci. U.S.A 92*, 7297−7301.

(2) Erbacher, P., Bettinger, T., Brion, E., Coll, J. L., Plank, C., Behr, J. P., and Remy, J. S. (2004) Genuine DNA/polyethylenimine (PEI) complexes improve transfection properties and cell survival. *J. Drug Targeting 12*, 223−236.

(3) Bolcato-Bellemin, A. L., Bonnet, M. E., Creusat, G., Erbacher, P., and Behr, J. P. (2007) Sticky overhangs enhance siRNA-mediated gene silencing. *Proc. Natl. Acad. Sci. U.S.A 104*, 16050−16055.

(4) Chollet, P., Favrot, M. C., Hurbin, A., and Coll, J. L. (2002) Side-effects of a systemic injection of linear polyethylenimine-DNA complexes. *J. Gene Med. 4*, 84−91.

(5) Moghimi, S. M., Symonds, P., Murray, J. C., Hunter, A. C., Debska, G., and Szewczyk, A. (2005) A two-stage poly(ethylenimine)-

mediated cytotoxicity: implications for gene transfer/therapy. *Mol. Ther. 11*, 990−995.
(6) Grandinetti, G., Ingle, N. P., and Reineke, T. M. (2011) Interaction of poly(ethylenimine)-DNA polyplexes with mitochondria: implications for a mechanism of cytotoxicity. *Mol. Pharm. 8*, 1709−19.
(7) Forrest, M. L., Koerber, J. T., and Pack, D. W. (2003) A degradable polyethylenimine derivative with low toxicity for highly efficient gene delivery. *Bioconjugate Chem. 14*, 934−940.
(8) Kim, Y. H., Park, J. H., Lee, M., Park, T. G., and Kim, S. W. (2005) Polyethylenimine with acid-labile linkages as a biodegradable gene carrier. *J. Controlled Release 103*, 209−219.
(9) Breunig, M., Lungwitz, U., Liebl, R., and Goepferich, A. (2007) Breaking up the correlation between efficacy and toxicity for nonviral gene delivery. *Proc. Natl. Acad. Sci. U.S.A 104*, 14454−14459.
(10) Knorr, V., Russ, V., Allmendinger, L., Ogris, M., and Wagner, E. (2008) Acetal linked oligoethylenimines for use as pH-sensitive gene carriers. *Bioconjugate Chem. 19*, 1625−1634.
(11) Prevette, L. E., Lynch, M. L., and Reineke, T. M. (2010) Amide spacing influences pDNA binding of poly(amidoamine)s. *Biomacromolecules 11*, 326−32.
(12) Miyata, K., Nishiyama, N., and Kataoka, K. (2012) Rational design of smart supramolecular assemblies for gene delivery: chemical challenges in the creation of artificial viruses. *Chem. Soc. Rev. 41*, 2562−2574.
(13) Wagner, E. (2012) Polymers for siRNA delivery: inspired by viruses to be targeted, dynamic, and precise. *Acc. Chem. Res. 45*, 1005−13.
(14) Schaffert, D., Badgujar, N., and Wagner, E. (2011) Novel Fmoc-polyamino acids for solid-phase synthesis of defined polyamidoamines. *Org. Lett. 13*, 1586−9.
(15) Schaffert, D., Troiber, C., Salcher, E. E., Frohlich, T., Martin, I., Badgujar, N., Dohmen, C., Edinger, D., Klager, R., Maiwald, G., Farkasova, K., Seeber, S., Jahn-Hofmann, K., Hadwiger, P., and Wagner, E. (2011) Solid-phase synthesis of sequence-defined T-, i-, and U-shape polymers for pDNA and siRNA delivery. *Angew. Chem., Int. Ed. Engl. 50*, 8986−9.
(16) Schaffert, D., Troiber, C., and Wagner, E. (2012) New sequence-defined polyaminoamides with tailored endosomolytic properties for plasmid DNA delivery. *Bioconjugate Chem. 23*, 1157−1165.
(17) Troiber, C., Edinger, D., Kos, P., Schreiner, L., Klager, R., Herrmann, A., and Wagner, E. (2013) Stabilizing effect of tyrosine trimers on pDNA and siRNA polyplexes. *Biomaterials 34*, 1624−33.
(18) Fröhlich, T., Edinger, D., Kläger, R., Troiber, C., Salcher, E., Badgujar, N., Martin, I., Schaffert, D., Cengizeroglu, A., Hadwiger, P., Vornlocher, H.-P., and Wagner, E. (2012) Structure−activity relationships of siRNA carriers based on sequence-defined oligo (ethane amino) amides. *J. Controlled Release 160*, 532−541.
(19) Martin, I., Dohmen, C., Mas-Moruno, C., Troiber, C., Kos, P., Schaffert, D., Lachelt, U., Teixido, M., Günther, M., Kessler, H., Giralt, E., and Wagner, E. (2012) Solid-phase-assisted synthesis of targeting peptide-PEG-oligo(ethane amino)amides for receptor-mediated gene delivery. *Org. Biomol. Chem. 10*, 3258−3268.
(20) Salcher, E. E., Kos, P., Frohlich, T., Badgujar, N., Scheible, M., and Wagner, E. (2012) Sequence-defined four-arm oligo-(ethanamino)amides for pDNA and siRNA delivery: Impact of building blocks on efficacy. *J. Controlled Release 164*, 380−6.
(21) Kos, P., Scholz, C., Salcher, E. E., Herrmann, A., and Wagner, E. (2013) Gene transfer with sequence-defined oligo(ethanamino)amides bioreducibly attached to a propylenimine dendrimer core. *Pharm. Nanotechnol. 1*, 269−281.
(22) Wightman, L., Kircheis, R., Rossler, V., Carotta, S., Ruzicka, R., Kursa, M., and Wagner, E. (2001) Different behavior of branched and linear polyethylenimine for gene delivery in vitro and in vivo. *J. Gene Med. 3*, 362−372.
(23) Kwok, A., and Hart, S. L. (2011) Comparative structural and functional studies of nanoparticle formulations for DNA and siRNA delivery. *Nanomedicine 7*, 210−9.
(24) Wang, R., Zhou, L., Zhou, Y., Li, G., Zhu, X., Gu, H., Jiang, X., Li, H., Wu, J., He, L., Guo, X., Zhu, B., and Yan, D. (2010) Synthesis and gene delivery of poly(amido amine)s with different branched architecture. *Biomacromolecules 11*, 489−95.
(25) Lin, C., Blaauboer, C.-J., Timoneda, M. M., Lok, M. C., van Steenbergen, M., Hennink, W. E., Zhong, Z., Feijen, J., and Engbersen, J. F. J. (2008) Bioreducible poly(amido amine)s with oligoamine side chains: Synthesis, characterization, and structural effects on gene delivery. *J. Controlled Release 126*, 166−174.
(26) Uchida, H., Miyata, K., Oba, M., Ishii, T., Suma, T., Itaka, K., Nishiyama, N., and Kataoka, K. (2011) Odd-even effect of repeating aminoethylene units in the side chain of N-substituted polyaspartamides on gene transfection profiles. *J. Am. Chem. Soc. 133*, 15524−32.
(27) Gao, Y., Yin, Q., Chen, L., Zhang, Z., and Li, Y. (2011) Linear cationic click polymers/DNA nanoparticles: in vitro structure-activity relationship and in vivo evaluation for gene delivery. *Bioconjugate Chem. 22*, 1153−61.
(28) Schaffert, D., Kiss, M., Rodl, W., Shir, A., Levitzki, A., Ogris, M., and Wagner, E. (2011) Poly(I:C)-mediated tumor growth suppression in EGF-receptor overexpressing tumors using EGF-polyethylene glycol-linear polyethylenimine as carrier. *Pharm. Res. 28*, 731−41.
(29) Lachelt, U., Kos, P., Mickler, F. M., Herrmann, A., Salcher, E. E., Rodl, W., Badgujar, N., Brauchle, C., and Wagner, E. (2014) Fine-tuning of proton sponges by precise diaminoethanes and histidines in pDNA polyplexes. *Nanomedicine NBM 10*, 35−44.
(30) Behr, J. P. (1997) The proton sponge: A trick to enter cells the viruses did not exploit. *Chimia 51*, 34−36.
(31) Sonawane, N. D., Szoka, F. C., Jr., and Verkman, A. S. (2003) Chloride accumulation and swelling in endosomes enhances DNA transfer by polyamine-DNA polyplexes. *J. Biol. Chem. 278*, 44826−44831.
(32) Benjaminsen, R. V., Mattebjerg, M. A., Henriksen, J. R., Moghimi, S. M., and Andresen, T. L. (2013) The possible ″proton sponge ″ effect of polyethylenimine (PEI) does not include change in lysosomal pH. *Mol. Ther. 21*, 149−57.
(33) Deshpande, M. C., Davies, M. C., Garnett, M. C., Williams, P. M., Armitage, D., Bailey, L., Vamvakaki, M., Armes, S. P., and Stolnik, S. (2004) The effect of poly(ethylene glycol) molecular architecture on cellular interaction and uptake of DNA complexes. *J. Controlled Release 97*, 143−56.
(34) Verma, A., and Stellacci, F. (2010) Effect of surface properties on nanoparticle-cell interactions. *Small 6*, 12−21.